Understanding the Quadrupole Mass Filter through Computer Simulation

Colin Steel and Michael Henchman
Department of Chemistry, Brandeis University, Waltham, MA 02254

A small portable mass spectrometer has been employed with great success in our undergraduate laboratory curriculum at Brandeis (*1*). The quadrupole mass spectrometer shows many advantages over the traditional magnetic-sector instrument and this is reflected in its popularity. It suffers, however, from one disadvantage. It is difficult to understand how a quadrupole mass spectrometer works. Beginning with the classic studies of Paul (*2*), many reviews have been written to explain the operation of the quadrupole and we cite only a few of them here (*3*–*8*). With some exceptions these accounts are mathematical and hard to follow. They do not help us to picture the motion of the ions in the complicated quadrupole field. We show here how the trajectories of the ions in the quadrupole can be very simply traced. By following these trajectories, we can understand how the quadrupole "works". We can change the parameters that control the quadrupole and we can see how this change affects the trajectories. We can understand these changes by analyzing the forces that act upon the ions—forces that vary with time. In this way we develop a pictorial understanding of the working of a quadrupole which is not evident from the mathematics.

The trajectories of the ions in the quadrupole cannot be traced experimentally nor can they be calculated analytically. They have to be computed. Trajectories may be traced as a student exercise in a straightforward way. The force acting on an ion is simple to specify and this defines the equations of motion in a differential form. Numerical integration then yields the position of the ion as a function of time, which is its trajectory.

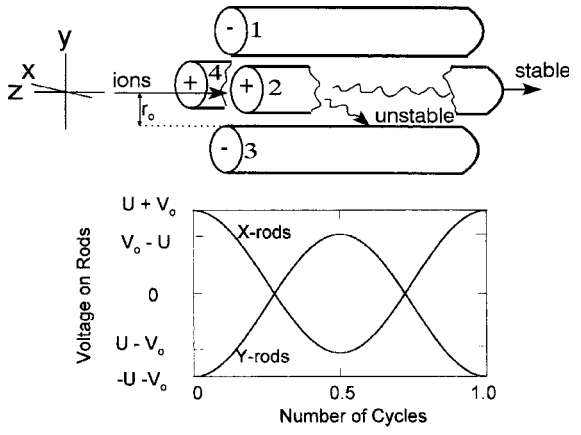

Figure 1. The quadrupole mass filter; the lower part of the figure shows the dc and rf voltages (U and V_o) applied to the rods. For the instrument described in ref *1*, the distance (r_o) from the central Z axis to the outer surface of a rod is 0.26 cm. The length (l) and diameter of the rods are 11 cm and 0.63 cm and the applied radiofrequency ($\omega/2\pi$) is 2.26 MHz.

The organization is as follows. In section 1 we describe the instrument and its parameters that can be varied. Section 2 gives a qualitative account of the operation of the quadrupole using main concepts: (i) moderate rf voltages stabilize a trajectory, (ii) large rf voltages destabilize a trajectory. In this section some results from later sections are quoted without proof. Section 3 develops the modeling of the trajectories. In section 4, we show how the form of the trajectories can be understood by analyzing the forces on an ion in the quadrupole field.

1. Description of the Quadrupole Mass Spectrometer

A schematic of the quadrupole is shown in Figure 1. Imagine singly charged positive ions being formed to the left of Figure 1. They are accelerated in the Z direction by a negative voltage, V_{accl}, typically ~20 volts. They enter the quadrupole close to the Z axis through a circular hole in a metal plate (not shown in Fig. 1) and the diameter of the hole defines the diameter of the ion beam entering the quadrupole field. To the right, ions that emerge from the quadrupole strike a detector and are measured as a current. Within the quadrupole, an ion experiences no forces in the Z direction: consequently, motion along the Z axis is not affected by the quadrupole field. Typical velocities in the Z direction [$v_Z = (2\ eV_{accl}/m)^{1/2}$] give flight times along the 11-cm quadrupole ranging from 25 to 1.8 μs as the ionic mass is varied from 200 to 1 amu. (Detailed instrumental parameters are given in the captions to Figs. 1 and 3.)

The quadrupole rods are connected diagonally in pairs. Within the region between the rods, they provide an electric field that affects the motion of the ions in the XY plane. As shown in Figure 1 the field is produced by applying dc and rf potentials to the rods,

$$\text{Rods on } Y\text{-axis: } V_1 = V_3 = -U - V_o \cos \omega t \qquad (1)$$

$$\text{Rods on } X\text{-axis: } V_2 = V_4 = +U + V_o \cos \omega t \qquad (2)$$

where U is the dc potential and V_o is the amplitude of the rf potential, applied at a fixed frequency $\omega/2\pi$ in the MHz range. With a flight time of 25 μs, an ion experiences about 50 rf cycles while traversing the quadrupole.

2. The Operation of the Quadrupole Mass Spectrometer

The working of a quadrupole mass spectrometer is complicated and our aim here is to bring the reader to a simple understanding. In section 2.1 we consider ions of a single mass m entering a quadrupole and we ask which voltages, U and V_o, let the ions be transmitted and which let them be deflected. We represent our findings on a plot of U against V_o, which is known as a *stability diagram* (Fig. 2). Unfortunately such a

stability diagram only applies to ions of a particular mass.

In section 2.2 we develop the *generalized stability diagram* (Fig. 4)—much more useful because it applies to all masses. The generalized diagram has two important applications. It reveals how the quadrupole can filter ions according to their mass-to-charge ratio (2.2.1) and it reveals how the quadrupole mass spectrometer can produce a mass spectrum (2.2.2).

In this section, we shall also examine the trajectories of ions in the quadrupole, obtained as described in section 3. The outcome of these trajectories—whether an ion is transmitted or deflected—enables us to draw the stability diagram. The detailed waveform of the trajectories (what the trajectories of the ions actually look like for different settings of U and V_o) reveals how the quadrupole works.

2.1. Ions of a Single Mass: the Stability Diagram

We start with the simplest possible case, a quadrupole with the radio frequency (ω) fixed and ions of only one mass (m). Only two controls can be varied, the dc voltage (U) and the rf amplitude (V_o). Therefore we ask: For what values of U and V_o will the quadrupole transmit the ions, allowing them to strike the detector and be recorded as a current? For what values will the ions be deflected, strike the rods, and be lost? To answer these questions, we could perform a large number of experiments, varying U and V_o and viewing the outcome (transmission or deflection). Our results would then be most simply expressed on a plot of U versus V_o (Fig. 2). Each experiment would be represented by a single point on this plot and in each case we would record the outcome. Our experiments would show that all ions with U and V_o values lying within the "triangle" in Figure 2 are transmitted; those lying outside the triangle are deflected to one of the rods.

Figure 2 is called a *stability diagram*. For ions to be transmitted through the quadrupole, their trajectories must be stable. When ions are deflected to a rod, their trajectories are unstable. The region within the stability diagram in which all trajectories are stable is roughly shaped like a triangle and may be called the "stability triangle". To understand the stability diagram we must examine the shapes of the trajectories in the various regions of the diagram. We obtain these trajectories by procedures developed in section 3. At this stage we cannot derive them but we can quote them and use them to understand the working of the quadrupole.

Consider the points C and D in Figure 3. These points lie within the stability triangle; their trajectories must be stable, and the ions must be transmitted. Figure 3 shows that the X and Y trajectories are all stable, as they should be. To "read" these trajectories, recall that the quadrupole does not act on the ion in the Z direction but only in the XY plane; and motion in the XY plane is traced most simply by two trajectories, one along the X axis and one along the Y. In each of the 10 trajectory diagrams the upper and lower boundaries correspond to rod surfaces. Since the velocity in the Z direction is constant, the horizontal axis in each diagram represents both the length of a rod and the time for an ion to traverse the filter.

We can now label the various regions of the stability diagram as unstable or stable (Fig. 2). Trajectories are stable within the stability triangle, requiring both the X and Y trajectories to be stable (Fig. 3, C and D). Outside the stability triangle, trajectories are unstable. This could result from instability of either the X trajectory or the Y trajectory. Once again, the trajectory calculations provide the answer.

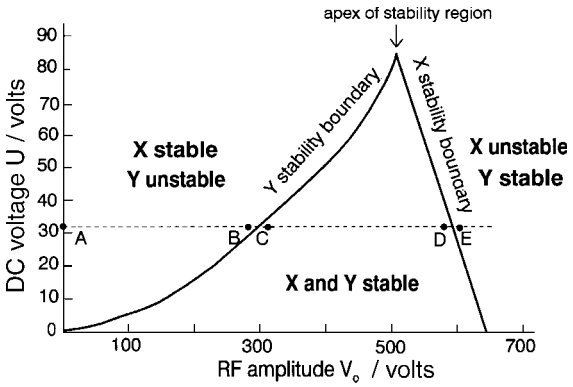

Figure 2. The stability diagram for a particular ionic mass in terms of the applied dc voltage (U) and rf amplitude (V_o). X and Y directions are defined in Figure 1 and are used throughout the text.

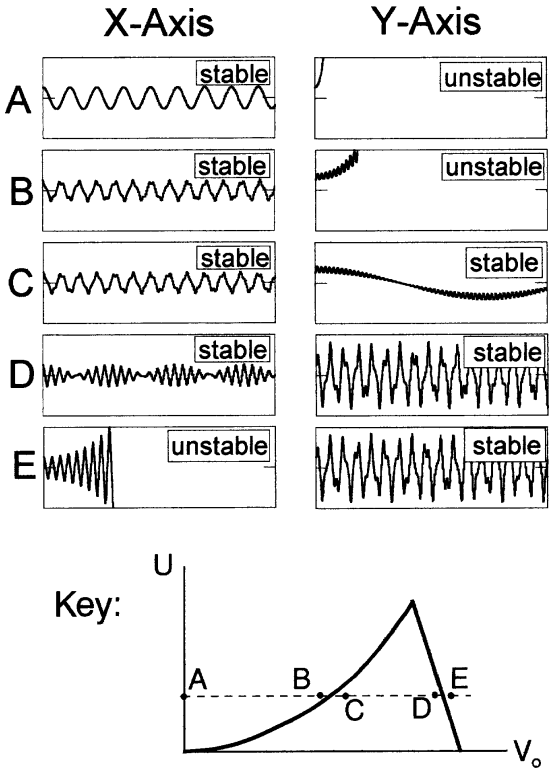

Figure 3. X and Y trajectories for the points A, B, C, D, E in Figure 2. Constant U (= 33 volts) and various V_o (0, 305, 310, 585, 590 volts). $x_o = y_o = 0.07$ cm, $r_o = 0.26$ cm, $L = 11$ cm, $m = 199$ amu, $\omega = 14.2 \times 10^6$ rad/s. $V_{accl} = 20$ V; time of flight through quadrupole = 25 μs.

Outside the triangle, at lower values of V_o, the Y trajectory is unstable and the X is stable, as shown by Figure 3, A and B. Complementing this, outside the triangle, at higher values of V_o, the X trajectory is unstable and the Y stable, as shown by Figure 3, insert E.

Finally, we can label the boundaries of the stability triangle. At lower values of V_o, moving inside the stability triangle from outside (Fig. 3, B → C), the Y trajectory changes from being unstable to stable and so the boundary is called the Y stability boundary. Likewise, for higher values of V_o, it is the X trajectory which changes from stable to unstable (Fig. 3, D → E) and the upper boundary of the stability triangle is called

the *X* stability boundary.

We ask the following general questions about the shape of the stability diagram. Why is the stability region shaped roughly like a triangle? Why does the *Y* stability boundary have a positive slope and the *X* stability boundary a steep negative one? Why are the *X* trajectories stable and the *Y* trajectories unstable at low rf voltages? Why do *X* trajectories (and ultimately *Y* trajectories) become unstable at high rf voltages? Answers to these questions come from a qualitative understanding of the stability diagram. To proceed, we must invoke two results developed in section 4:

a. Low rf voltages stabilize the trajectory; and
b. High rf voltages destabilize the trajectory.

The first seems counterintuitive. As the rf voltage on a rod switches from negative to positive, a positive ion will be first attracted, then repelled. Intuition suggests that these two effects should cancel but actually they don't. As we shall see in section 4 and from Figure 5, the overall effect is to drive the ion towards the central *Z* axis and stabilize the trajectory.

The second is simpler to grasp. Large rf voltages induce large oscillations in the motion of the ion about the *Z* axis and the increasing amplitude in the motion causes the ion ultimately to strike a rod. Again an analysis is given later in section 4 and displayed in Figure 6.

Using these two concepts, we now explore the features of the stability diagram by moving along the line A → B → C → D → E in Figures 2 and 3 (where *U* is fixed). Point A is simple to analyze and we use *a* and *b* (above) to analyze the rest.

Point A represents the situation of an ion in a dc field with the rf switched off. In general the ion will not be located exactly on the *Z* axis. Rods 2 and 4, at a positive dc voltage, will *repel* the positive ion, causing it to oscillate in the *X* direction. *X* motion is therefore stable (Fig. 3, trajectory A [*X*]). Rods 1 and 3, at a negative dc voltage, will *attract* the positive ion, which will move toward and strike whichever rod is closer. *Y* motion is therefore unstable (Fig. 3, trajectory A [*Y*]). Note that the *X* stability and *Y* instability are shown in the stability diagram (Fig. 2).

We now move A → B → C. The rf voltage is increasing but still low, so that its action is *stabilizing* (*a*). At A, the *X* motion is stable; moving to C, it becomes more so. At A, the *Y* motion is unstable with the briefest of flight times; at B, it has been stabilized a little, still unstable but with a longer flight time; and at C, the stabilizing rf field has made the trajectory stable. At B, the *Y* motion is still just unstable and at C, just stable, with the switchover occurring at the *Y* stability boundary. The larger the initial dc voltage, the larger the rf voltage needed to offset it. For that reason, the *Y* stability boundary has a positive slope. Traces of the *X* and *Y* trajectories for A, B, and C validate this description (Fig. 3).

We now move C → D → E. The rf voltage is still increasing but is now large, so that its action is *destabilizing* (*b*). At C, both *X* and *Y* motions are stable: ultimately both must become unstable. The *X* motion becomes unstable at a lower voltage (Fig. 3, trajectories E [*X*] and E[*Y*]). Again, traces of the *X* and *Y* trajectories for C, D, and E validate this description (Fig. 3). The switchover from *X* stable to *X* unstable occurs at the *X* stability boundary, which has a steep negative slope (Fig. 2). In section 4 we shall find that in the case of *X* motion, the dc potential (*U*) reinforces the large rf potential (V_o) in driving the ion towards the *X* rods; hence as *U* increases the value of V_o required to obtain *X* instability decreases, resulting in a negative slope for the *X* stability boundary. The steepness of the slope is associated with the fact that the value at which the *X* motion becomes unstable depends mainly on the large rf voltage (V_o) and, to first approximation, is independent of the relatively modest dc voltage.

The stability diagram describes the working of the quadrupole for ions of a single mass. We now generalize the description for ions of all masses in terms of the generalized stability diagram. This involves only rescaling the axes; the shape of the diagram remains unchanged.

2.2. Ions of All Masses: the Generalized Stability Diagram

For ions of a single mass, the stability diagram describes the range of quadrupole settings, *U* and V_o, which cause the ion to be deflected or transmitted. For each different mass, there is a different stability diagram. We need one diagram that will work for all masses. Theory (derived in section 3.1) tells us to replace the variables *U* and V_o by new variables α and *q*, which we can think of as U/m and V_o/m. There are other terms in α and *q* (eqs 3 and 4) but they can be ignored because they are constant.

When we make an α versus *q* plot, we obtain the *generalized stability diagram* (Fig. 4), which applies to all masses (strictly, all mass-to-charge ratios). Its universal applicability is shown by the location of the apex, which is always at the (α, *q*) point (0.237, 0.706). Again the *X* stability boundary always terminates at the (α, *q*) point (0, 0.91). Using the generalized stability diagram it is easy to show how the quadrupole works as a mass-to-charge ratio filter and how it can deliver a mass spectrum.

2.2.1. The Quadrupole as a Mass Filter

Again we restrict discussion to singly charged ions. For a quadrupole to function as a mass filter with unit mass resolution, it must be able to separate mass *m* from mass (*m* – 1) and lower masses, and from mass (*m* + 1) and higher masses. That is, we have to be able to tune the quadrupole so that

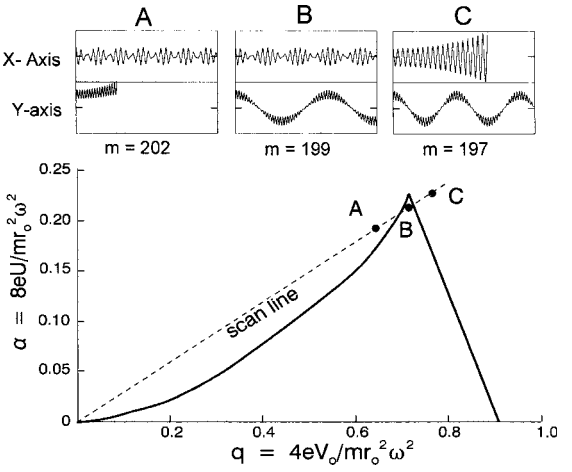

Figure 4. Generalized stability diagram in terms of the dimensionless parameters α and *q*. The three inset diagrams show *X* and *Y* trajectories for *m* = 202, 199, and 197 amu in the regions exhibiting (A) *Y* instability, (B) no instability, and (C) *X* instability. For all insets *U* = 82 volts and V_o = 497 volts, V_{accl} = 20 volts, r_o = 0.26 cm, $x_o = y_o$ = 0.1 cm, *L* = 11 cm, ω = 14.2×10^6 rad/s.

mass m lies within the stability triangle, whereas all other masses, (m – 1) and lower and (m + 1) and higher, do not. How can we do this? We could tune mass m to the tip of the apex of the generalized stability diagram (Fig. 4) because most of the surrounding points lie outside the stability diagram. In principle, that is a good idea; in practice it isn't, because random voltage fluctuations in U and V_o would move the mass m in and out of the stability triangle. In practice we tune it not to the apex (α = 0.237; q = 0.706) but slightly below, say to point B in Figure 4 (α = 0.233; q = 0.706), where noise will not kick the ion of mass m out of the triangle.

With the quadrupole tuning mass m to the point B (Fig. 4), we now check on masses (m – 1) and (m + 1). If they lie outside the stability triangle, the quadrupole can act as a mass filter. If they lie inside, mass m will not be selected from masses (m – 1) and (m + 1) .

We start by calculating the quadrupole voltages needed to focus the mass m on the point B. We call these values U and V_o. By using the equations that define α and q (section 3) and substituting the values of α and q that define the point B, we can evaluate U and V_o,

$$\alpha = 8\,eU/mr_o^2\omega^2 = 0.233 \qquad (3)$$

$$q = 4\,eV_o/mr_o^2\omega^2 = 0.706 \qquad (4)$$

We now ask, with the quadrupole tuned at voltages U and V_o, where the (singly charged) masses (m – 1) and (m + 1) will appear on the stability diagram.

Let's start with mass (m – 1). We want to locate its position on Figure 4 (i.e., its α and q values). These are given by eqs 5 and 6:

$$\alpha = 8\,eU/(m-1)r_o^2\omega^2 \qquad (5)$$

$$q = 4\,eV_o/(m-1)r_o^2\omega^2 \qquad (6)$$

Notice that the α and q values for mass (m–1) are both larger by the same factor, $m/(m-1)$, than those for mass m at point B. Since the ratio (α/q) is fixed (by the tuning of m to B), mass (m – 1) will be located on the straight line drawn through the origin and passing through B… somewhere in the vicinity of point C. The corresponding values for mass (m + 1) will be smaller, placing it on the same straight line but now below B… somewhere in the vicinity of point A. The straight line on which these masses lie is called the *scan line.* Clearly, for given values of U and V_o all masses lie on the same scan line.

To investigate if a particular quadrupole can function as a mass filter in a particular case, we must establish whether points A and C lie inside or outside the stability triangle. In section 3 we use the trajectories shown in Figure 4 to establish the resolution that can be achieved.

2.2.2. Running a Mass Spectrum on the Quadrupole

The above discussion tells us that to maximize resolution, each mass must progressively be brought to point B in Figure 4. When any particular mass is being measured, all the other masses will be strung out along the scan line, the heaviest closest to and the lightest furthest from the origin. To run a mass spectrum, we move all the masses progressively through point B. This is done by starting at a low value for U and V_o and progressively increasing both while keeping the ratio U/V_o constant at $^1/_2$(0.233/0.706) throughout.

3. Computer Modeling

In this section we show how the performance of the quadrupole may be analyzed under any conditions by examining the trajectories of the ions, which are readily obtained by computer simulation. The first step is to derive the equations governing the motion of the ions. Although these equations may be found in other references (*2–5, 7, 8*), they are repeated here for convenience and completeness.

3.1. Theoretical Background

The dc and rf voltages determine the potential in the X–Y plane in the charge-free region between the rods and the potential (V) there must satisfy the two-dimensional Laplace equation (*9, 10*) $\partial^2V/\partial x^2 + \partial^2V/\partial y^2 = 0$. The simplest equation satisfying this differential equation is, $V(x,y) = (x^2 - y^2)\cdot K$ where K is some constant determined by the boundary conditions. The internal surfaces of the rods mark the edge of the charge-free region and fix the boundary conditions on the X and Y axes so that

$$V(-r_o,0) = V(r_o,0) = (U + V_o\cos\omega t)$$

and

$$V(0,-r_o) = V(0,r_o) = -(U + V_o\cos\omega t)$$

so that $K = (U + V_o\cos\omega t)/r_o^2$. Thus,

$$V(x,y) = (x^2 - y^2)(U + V_o\cos\omega t)/r_o^2 \qquad (7)$$

We see from eq 7 that an equipotential curve within the quadrupole, that is, $V(x,y)$ = const, has the form of a rectangular hyperbola. Indeed, early quadrupoles were constructed using rods having hyperbolic surfaces (*2, 6*). But in practice this was found to be unnecessary, and rods circular in cross-section, which are much more easily fabricated, are now used.

The force in the X direction on an ion, charge e, at (x,y) is $F_x = -e\,\partial V/\partial x$, with a similar formula for the force F_y in the Y direction. These equations for F_x and F_y in conjunction with Newton's second law (force = mass · acceleration) and eq 7 immediately yield

$$F_x = m\cdot d^2x/dt^2 = -2e(U + V_o\cos\omega t)x/r_o^2 \qquad (8)$$

$$F_y = m\cdot d^2y/dt^2 = 2e(U + V_o\cos\omega t)y/r_o^2 \qquad (9)$$

Notice that, since there are no cross terms, the motions in the X and Y directions are independent. This justifies displaying ion trajectories as independent X and Y paths in Figures 3 and 4. Equations 8 and 9 are second-order differential equations. Generally they are recast (*4*) into dimensionless form by using the substitutions

$$\phi = \omega t/2 \qquad (10)$$

$$\alpha = 8eU/r_o^2m\omega^2 \qquad (3')$$

$$q = 4eV_o/r_o^2m\omega^2 \qquad (4')$$

in which case they become

$$d^2x/d\phi^2 = -(\alpha + 2q\cos 2\phi)x \qquad (8')$$

$$d^2y/d\phi^2 = (\alpha + 2q\cos 2\phi)y \qquad (9')$$

The parametric dependence of α and q on m/e emphasizes again that the quadrupole sorts ions according to their mass-to-charge ratio.

Finally, the equivalent three-dimensional Laplace equation $\partial^2V/\partial x^2 + \partial^2V/\partial y^2 + \partial^2V/\partial z^2 = 0$ is the fundamental equation for the quadrupole storage ion trap (*2, 5, 7*) and an essentially

similar theory applies to these devices.

3.2. Trajectory Generation

To generate ion trajectories, we have to integrate the differential equations of motion (8 and 9). Direct integration to provide analytical solutions for the ion trajectories is not possible: instead, they are derived very easily by numerical integration, using a few lines of computer code. To do so we first recast eqs 8 and 9 in first-order form, defining $u = dx/dt$ and $v = dy/dt$ as the velocities in the X and Y directions:

$$du/dt = -2e(U + V_o \cos \omega t)\, x/mr_o^2 = f(t,x) \qquad (11)$$

$$dv/dt = 2e(U + V_o \cos \omega t)\, y/mr_o^2 = g(t,y) \qquad (12)$$

Numerical integration by the Euler method (*11*, *12*) starts at an initial state (u_o, v_o, x_o, y_o, t_o). A time interval dt generates a new state (u_1, v_1, x_1, y_1, t_1). This is repeated n times. The trajectory of the ion is then represented by the set (x_i, y_i, t_i), where $i = 0, 1, \ldots, n$. We have to make assumptions about the initial conditions. At time zero ($t_o = 0$) we assume that $u_o = v_o = 0$ and that the ion enters the quadrupole off axis at the point (x_o, y_o). In passing from (u_o, v_o, x_o, y_o, t_o) to (u_1, v_1, x_1, y_1, t_1), changes du_o, dv_o, dx_o, dy_o, dt_o occur such that $u_1 = u_o + du_o$, etc. The incremental changes are estimated as follows: $du_o = f(t_o, x_o)dt$; $dv_o = g(t_o, y_o)dt$; $dx_o = u_o dt$; $dy_o = v_o dt$; $dt_o = dt$. Better estimates of these increments are given by the 4th-order Runge–Kutta method (*11*, *12*), which was employed throughout this study in implementing the numerical integration. The time interval (dt) was typically a factor of 30 less than the period ($2\pi/\omega$) of the rf field. The upper limit of integration is given by the flight time of the ion through the quadrupole, which is determined from the value of v_Z and L.

Using a 486 PC and uncompiled QuickBasic, such a program takes less than two seconds to run and display the trajectories on the monitor, so a student can quickly change experimental parameters and view the results.

This allows for ready experimentation to examine how a quadrupole "works":

1. For the conditions shown in Figure 4 the mass range that gets through the filter is about 199 ± 2.25, so that the resolution is $m/\Delta m = 199/2.25 \approx 88$. This agrees well with the value obtained from the empirical formula (*5*) $m/\Delta m = 0.357/(0.237 - \alpha_{0.706})$, where $\alpha_{0.706}$ is the value of α at the point of intersection of the scan line with $q = 0.706$. Lowering α/q (or U/V_o) even modestly can result in a serious loss of resolution. Thus, when α/q is lowered by 10% to 0.30 the resolution drops to ≈ 12. By changing U and V_o so as to tune in a new mass to point B (Fig. 4) and tracing new trajectories, the student can show that the resolution $m/\Delta m$ is independent of m and depends only on the value of $\alpha_{0.706}$.
2. In Figure 3 we showed how for a given mass and at constant dc potential (U) the points on the Y and X stability boundaries could be obtained by systematically increasing V_o and looking at the values of V_o at which the changes from Y unstable to Y stable and from X stable to X unstable occur. By varying U and repeating this procedure the stability diagram may be mapped.
3. Other factors that can influence the resolving power of a quadrupole (*5*), such as ω, the initial values x_o, y_o, the rod length L, and the rod separation ($2r_o$) are quite subtle and require a more detailed analysis, accounting for the fact that not all ions will start with $u_o = v_o = 0$.

4. Detailed Description of the Trajectories

In this section, a closer examination of the forces on an ion and the resulting trajectories elucidates and clarifies the main concepts used in section 2: (i) moderate rf voltages are stabilizing, and (ii) large rf voltages are destabilizing.

4.1. Moderate RF Voltages Are Stabilizing

The upper part of Figure 5 shows a stable Y trajectory of an ion when $U = 0$ and $V_o = 100$ volts; notice the absence of a dc potential, so the ion is subject to only a rf field. The main diagram shows a detail of this trajectory during the first 1.5 μs. Also shown as the dotted curve is the force on the particle (F_y) according to eq 9. Since $y > 0$, this equation shows that F_y oscillates with the same frequency (ω) as the rf potential on the Y rods.

At $t = t_1$ the particle is moving toward a Y rod, but during the interval $[t_1,t_2]$ the ion reverses direction because it suffers an impulse ($= \int_{t_1}^{t_2} F_y dt$) that is directed towards the central Z axis (a stabilizing impulse). During the next interval ($[t_2,t_3]$) the impulse changes direction towards a Y rod (a destabilizing impulse). However, since the particle is now closer to the axis than during the previous interval and since F_y depends upon y, the magnitude of the impulse during $[t_2,t_3]$ is less than during the preceding interval $[t_1,t_2]$. Thus the particle is subjected to a series of impulses that are stabilizing, destabilizing, stabilizing, …, and in which each destabilizing impulse is smaller that the preceding stabilizing impulse. The direction and magnitude of these impulses is represented by the arrows attached to the Y trajectory. The net result of this train of impulses is stabilization and the overall motion of the particle is toward the center. This results in the low-frequency oscillation about the central Z axis with a period of about 8.5 μs, which can be seen in the full trajectory.

Returning to the central detail, we see that superimposed

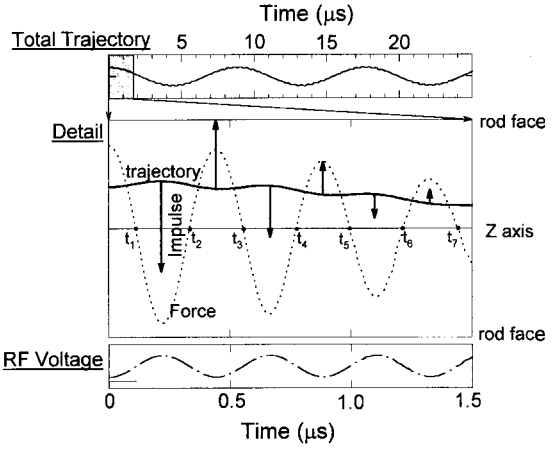

Figure 5. Stable Y trajectory obtained at $U = 0$ volts, $V_o = 100$ volts, and $m = 199$ amu; other parameters as for Figure 4. The upper part of the figure shows the trajectory through the entire filter. The full line in the detail is an enlargement of this trajectory during the initial 1.5 μs (shaded area of total trajectory). The lowest section shows the voltage on the Y rods. This voltage results in the oscillating force (arbitrary units) shown as a dotted curve in the main detail. The force imparts successive impulses (shown as a series of arrows) on the ion, driving the ion toward the center.

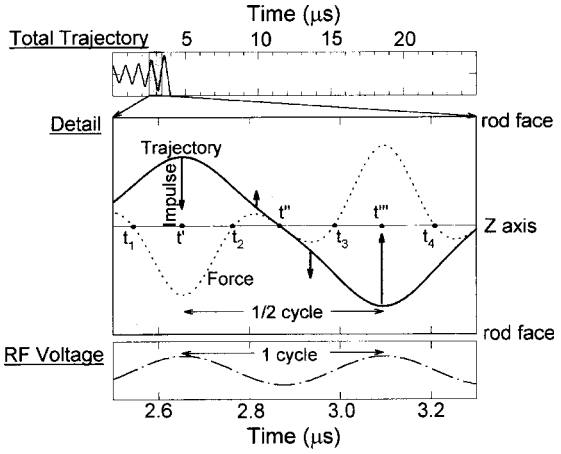

Figure 6. Unstable *X* trajectory obtained at $U = 0$ volts, $V_o = 647$ volts, and $m = 199$ amu; other parameters as for Figure 4. The upper part of the figure shows the total trajectory. The full line in the detail is an enlargement of this trajectory during the small initial section shown as the shaded area in the total trajectory. The lowest part of the diagram shows the voltage on the *X* rods. This voltage results in the oscillating force (arbitrary units) shown as a dotted curve in the main detail. The force imparts successive impulses (shown as a series of arrows) on the ion, driving it toward a rod with ever-increasing amplitude and an oscillation frequency equal to 1/2 the radio frequency.

on this low-frequency motion, the trajectory exhibits a high-frequency oscillation that has the same frequency as F_y and so must also equal the rf frequency ω. These two frequencies can also be clearly seen for the *Y* trajectory in Figure 4 insert B.

4.2. Large RF Voltages Are Destabilizing

The upper part of Figure 6 shows the total *X* trajectory of an ion when *U* is still zero but now the rf amplitude (V_o) has been increased from 100 to 647 volts. The central diagram shows an enlargement during an early part of the trajectory. Also shown, as the dotted curve, is the force on the particle (F_x) according to eq 8. As in the previous figure, at t_1 the particle is moving toward a rod and during the interval $[t_1,t_2]$ the ion reverses direction because of the impulse $\int_{t_1}^{t_2} F_x dt$ directed toward the central axis. However, in this case V_0 is sufficiently large, and consequently the magnitude of the impulse sufficiently great, that during the next interval ($[t_2,t'']$) the particle is driven close to the central axis. Because *x* is now small, eq 8 tells us that the force (and also the impulse) must be small and is not able to reverse the direction of the ion. In fact at t'' the force is zero, since $x = 0$. Although the two impulses during $[t_2,t'']$ and $[t'',t_3]$ are small, they play a crucial role. If the magnitude of the impulse during $[t'',t_3]$ is greater than the magnitude of the impulse during $[t_2,t'']$, the ion will be driven closer to an *X* rod at the turning point t''' than at the prior turning point, t'. That is, the amplitude is increasing and the trajectory is unstable, as can be seen from the total trajectory.

On the other hand, if the position of t'' is moved to the right by decreasing V_o (and thus the magnitude of the impulse $\int_{t_1}^{t_2} F_x dt$), then we may have $(t'' - t_2) > (t_3 - t'')$, so that the magnitude of the impulse during $[t_2,t'']$ becomes greater than the magnitude of the impulse during $[t'',t_3]$. In this case the position of the particle at t''' will be farther from the *X* rod than at t'. In this case the amplitude will decrease and the trajectory would still be stable. Clearly the *X* stability boundary condition is obtained when $(t'' - t_2) = (t_3 - t'')$. Such a change from an unstable to a stable *X* trajectory can be seen by looking at Figure 3, E and D.

Finally, observe that, although the rf period is $(t_3 - t_1)$, the period for the high-frequency *X* oscillation is $2(t''' - t') = 2(t_3 - t_1)$. That is, the high-frequency *X* oscillation occurs at not at ω, as for the stable *Y* oscillation, but at ω/2. The difference in the high-frequency *X* and *Y* oscillations can be clearly seen in Figure 4C.

4.3. Instability of the *Y* Trajectory at High RF Voltages

In Figures 2 and 3 we referred to a situation in which the dc voltage was held constant at $U = 33$ volts. The *Y* trajectory is unstable A → B, stable C → D → E, and must become unstable again at still higher rf voltages (recall concept *b*). Why is a higher rf voltage ($V_o \approx 695$ volts) required to destabilize a *Y* trajectory than an *X* trajectory ($V_o \approx 650$ volts)? This result seems paradoxical in view of the fact that in the absence of rf voltage, the dc voltage stabilizes the *X* trajectory and destabilizes the *Y* trajectory (Fig. 3A).

The answer is to be found in Figure 6. For *X* motion during the period $[t_1,t_2]$, the rf and dc voltages *reinforce*. This means that the ion can receive a sufficiently large turning moment during this time so that the ion is driven to the center and can satisfy the condition $(t'' - t_2) = (t_3 - t'')$ for the *X* stability boundary at relatively small V_o. During the same period, for *Y* motion the rf and dc voltages *oppose*; so to get the rf voltage large enough to counteract the dc voltage, V_o has to be increased over its value for *X* motion.

Acknowledgments

C.S. thanks the Research Corporation for support under grant DS-99 and M.H. thanks the Dreyfus Foundation for support during the writing of this paper.

Literature Cited

1. Henchman, M.; Steel, C. *J. Chem. Educ.* 1998, *75*, 1042–1049.
2. Paul, W. *Angew. Chem. Int. Ed. Engl.* 1990, *29*, 739.
3. Miller, R. E.; Denton, M. B. *J. Chem. Educ.* 1986, *63*, 617.
4. Kiser, R. W. *Introduction to Mass Spectrometry and Its Applications;* Prentice-Hall: Englewood Cliffs, NJ, 1965.
5. Lawson, G.; Todd, J. F. J. *Chem. Br.* 1972, *8*, 373.
6. Denison, D. R. *J. Vac. Sci. Technol.* 1971, *8*, 266.
7. March, R. E.; Hughes R. J. *Quadrupole Storage Mass Spectrometry*; Wiley: New York, 1989; Chapter 2.
8. Leary, J. J.; Schmidt, R. L. *J. Chem. Educ.* 1996, *73*, 1142.
9. Duckworth, H. E. *Electricity and Magnetism*; Holt, Rinehart and Winston: New York, 1961; Chapter 2.
10. Hirst, D. M. *Mathematics for Chemists*; MacMillan: London, 1976; Chapter 11.
11. Noggle, J. H. *Physical Chemistry on a Microcomputer*; Little Brown: Boston, 1985; Chapter 9.
12. Press, W. H.; Flannery, B. P.; Teukolsky, S. A.; Vetterling W. T. *Numerical Recipes*; Cambridge University Press: Cambridge, 1986; Chapter 15.